Time-resolved reflectivity measurements on silicon and germanium using a pulsed excimer KrF laser heating beam

G. E. Jellison, Jr., D. H. Lowndes, D. N. Mashburn, and R. F. Wood
Solid State Division, Oak Ridge National Laboratory, Oak Ridge, Tennessee 37831
(Received 7 March 1986)

Time-resolved reflectivity measurements on silicon and germanium have been made during pulsed KrF excimer laser irradiation (248 nm). The reflectivity was measured simultaneously with probe-laser wavelengths of 632.8 and 1152 nm, and the energy density of each laser pulse was recorded. From these measurements, we were able to determine the reflectivity of the hot solid just before the onset of melting, the reflectivity of the melt, the melt duration, and the time of the onset of melting. Melting-model calculations were also performed, with the reflectivity of solid and liquid Si and Ge treated as parameters for fitting the experimental values of the melt duration and the time of the onset of melting. The resulting parameter values are in agreement with those obtained from self-reflectivity measurements. Near the melting threshold, it was observed that the melt duration was never less than 20 ns for Si and 25 ns for Ge, while the maximum reflectivity increased from its value for the hot solid to that for the liquid over a finite energy range. These results, together with a reinterpretation of time-resolved ellipsometry measurements, indicate that, during the melt-in process, the near-surface region does not melt homogeneously, but rather consists of a mixture of solid and liquid phases.

I. INTRODUCTION

Pulsed-laser melting of semiconductors has been the subject of extensive study for the last 7 to 8 years and the nature of the pulsed-laser annealing process is well established: If a light pulse of sufficient energy density E_l is incident upon the surface of a semiconductor, the near-surface region of the sample will melt.[1] The time of onset of melting and the melt duration depend in a complicated fashion on the materials properties and on the parameters of the laser pulse, including its wavelength, pulse duration and shape, and E_l. Melting-model calculations[2] have been carried out to describe the results of time-resolved reflectivity measurements on Si using a ruby laser,[2-4] and a Nd:YAG frequency-doubled laser[5] (here YAG denotes yttrium aluminum garnet), as well as the results of time-resolved electrical conductivity measurements using a ruby laser.[6]

Throughout the study of the pulsed-laser annealing process, time-resolved optical measurements have played a central role. The earliest time-resolved reflectivity (TRR) measurements were carried out by Sooy *et al.*,[7] where they found that the reflectivity underwent a large increase which lasted for several tens of nanoseconds after laser irradiation and was attributed to a phase change to a metallic state. Later TRR experiments by Auston *et al.*[8] attributed the increase in reflectivity to the melting of the semiconductor surface, since liquid semiconductors generally are metallic and therefore will have a higher reflectivity than the hot, solid semiconductor at the same probe wavelength (632.8 nm for the experiments of Auston *et al.*). However, the reflectivities measured by Auston *et al.* for 632.8-nm light polarized perpendicular and parallel to the plane of incidence were significantly lower than those determined from the ellipsometry measurements of Shvarev *et al.*[9]

In a later set of experiments Lowndes *et al.*[3] and Lowndes[4] examined the TRR as well as the time-resolved transmission (TRT) of silicon irradiated with a ruby laser. It was found that the transmission through the silicon sample went to zero at the same time that the reflectivity increased to the high-reflectivity value, consistent with the near-surface region undergoing a phase transition to a metallic state. Another result of these experiments was that the normal-incidence reflectivity of the high-reflectivity phase was measured to be 72%, in close agreement with the value of 73% determined from the results of Shvarev *et al.*;[9] in these experiments, great care was taken to properly focus the probe-laser beam and to use collection optics in order to collect all the reflected light. The results of the TRR and TRT measurements compared well with melting-model calculations. Lowndes *et al.*[5] performed TRR measurements of silicon during irradiation with a frequency-doubled Nd:YAG laser. In this set of experiments, the time of the onset of melting was also measured and by comparison with model calculations, was found to be very sensitive to the optical and thermal properties of the hot, solid material just before it melts. It was concluded that the absorption coefficient at the wavelength of the frequency-doubled Nd:YAG laser (532 nm) must be intensity dependent.

Recently, Jellison and Lowndes[10] performed time-resolved ellipsometry (TRE) measurements during the pulsed-laser irradiation of silicon with an excimer (KrF, wavelength of 248 nm) laser, using a 632.8-nm probe-laser wavelength. From these measurements, they concluded that the optical constants of liquid silicon at 632.8 nm were given by $n=3.8$ and $k=5.2$ (resulting in a normal-incidence reflectivity of 71.5%), in minor disagreement with the results of Shvarev *et al.*[9] In addition, they were able to determine the effective surface temperature for hot, solid silicon before and immediately after the molten

phase, which indicated that the hot solid reached $\sim 1400\,^{\circ}C$ before undergoing the phase transition.

In this paper, we present the results of TRR measurements during pulsed KrF (248 nm) excimer laser irradiation of both silicon and germanium. The TRR measurements were performed at two different probe-laser wavelengths (632.8 and 1152 nm), using cw lasers focused on the same spot. From these measurements, we are able to determine the following: (1) duration of the melt as a function of laser-energy density, (2) time of onset of melting as a function of laser-energy density, (3) reflectivity of the hot solid just before the onset of melting for both Si and Ge at 632.8 and 1152 nm, and (4) reflectivities of Si and Ge in the liquid phase at 632.8 and 1152 nm.

An excimer laser has several advantages over solid-state lasers (such as ruby or Nd:YAG) for TRR measurements and the subsequent interpretation: (1) The energy density and pulse shape are reasonably constant from pulse-to-pulse ($\sim 5\%$) and, with care, the energy density of each laser pulse can be monitored to 2%. (2) Because excimers are multimode lasers, the transverse homogeneity of the laser beam is very good (we measure ours to be $\pm 5\%$ for an aperture size of 50 μm), without using bent light rods or diffuser plates. (3) Since the excimer laser radiation is in the uv, the absorption coefficient for most semiconductors is very large ($> 10^6$/cm), and is effectively taken out of the experiment. The one disadvantage of excimer lasers for TRR measurements is that the reflectivities of semiconductors in both the hot, solid and liquid states are large but not precisely known at the excimer wavelengths. We give the results of melting-model calculations, where the reflectivities of the solid and liquid states have been used as fitting parameters to determine the time of the onset of melting and the melt duration. Self-reflectivity (the reflectivity of the pump excimer radiation) measurements of Si and Ge during pulsed KrF laser irradiation allowed us to determine the ratios of the reflectivities of the hot solid to those of the liquid. A comparison of these results with the reflectivities determined using the melting-model calculations showed good agreement.

In studying the TRR of Si during pulsed excimer laser irradiation, Jellison *et al.*[11] found that the maximum reflectivity increased monotonically with E_l for values just above the melting threshold. In this work, we present the details of these measurements on Si, as well as results on Ge. The interpretation requires that the melt-in process be considered inhomogeneous; that is, melting does not occur at a well-defined planar melt front, but rather the front-surface region consists of a mixture of solid and liquid, where the fraction of liquid and the thickness are time dependent. Also, we present a reinterpretation of the TRE experiments of Jellison and Lowndes,[10] which allows us to quantify the fraction of solid and the depth of the solid-liquid mixture as a function of time. The implications of these results for melting-model calculations are briefly considered.

II. EXPERIMENT

The Lambda-Physik 210 KrF excimer laser (248 nm = 5 eV) used for the experiments has a pulse width of ~ 38 ns full width at half maximum and can produce up to 1.3 J/pulse. Energy densities up to 1.8 J/cm^2, uniform to $\sim 5\%$ over an area ~ 3 mm in diameter, were obtained by focusing the incident laser beam. A typical time profile of the pulse from this laser is shown in the bottom panel of Fig. 1, although it was observed that there were slight differences in the pulse shape depending upon the transverse position in the laser beam. A beam splitter (Suprasil polished on both sides) was placed in front of the sample to monitor the energy of each laser pulse with a microjoule meter, which was interfaced to a laboratory computer.

The silicon samples used were 5 Ω cm n-type float-zoned silicon wafers cut on the 100 face and polished. Three germanium samples were used: (1) 0.1 Ω cm, p-type, cut on the (111) face; (2) 0.1 Ω cm, p-type, cut on the 100 face; and (3) high-purity ($\sim 10^9$ electrically active sites per cm^3), p-type, cut on the (111) face, supplied by ORTEC, Oak Ridge, TN. No difference in the TRR was observed among the three different Ge samples.

During the course of these experiments, it was found that it was necessary to clean all samples with appropriate solvents to remove any organic surface contaminants just before the experiment. In addition, it was necessary to remove the surface oxide from the Ge samples within a few hours of the experiment, because Ge tends to oxidize

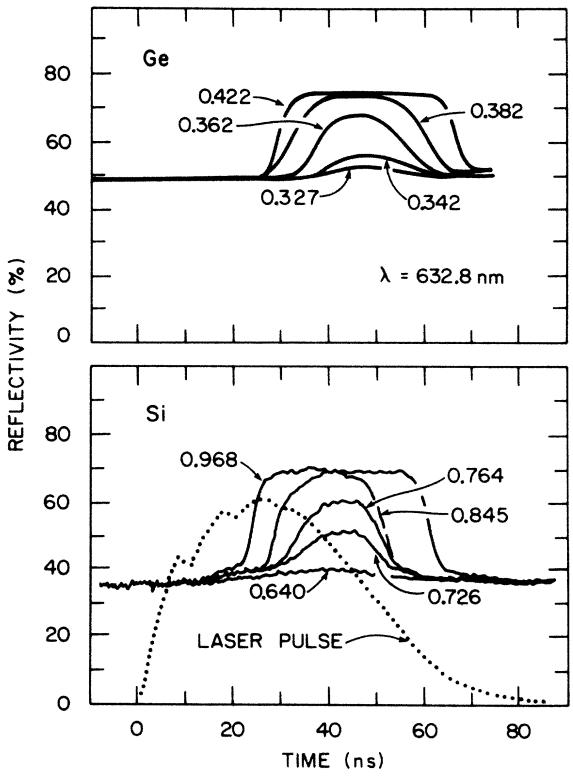

FIG. 1. Time-resolved reflectivity of Ge (top panel) and Si (bottom panel) at 632.8 nm during pulsed KrF excimer laser irradiation. The time profile of the laser pulse is shown in the bottom panel, for which the y axis is in arbitrary units. The numbers in the figure refer to the energy density in J/cm^2 of the laser pulse.

quickly, and the Ge oxide (unlike SiO_2) is not transparent to the 248-nm light.[12] In addition, excimer laser irradiation of Ge with energy densities large enough to melt the front surface region results in a significant growth of oxide. (~ 100 shots of excimer radiation on Ge with an energy density of ~ 0.4 J/cm^2 results in ~ 80 nm of oxide.) Therefore, we were careful to irradiate each spot on the sample only once. Although this problem is much less important for the case of silicon, the same precaution was taken for the silicon experiments.

The two probe-laser beams of 632.8 and 1152 nm were coincident on the sample surface (within ~ 30 μm) and were focused to a spot size < 50 μm in diameter. The reflected light was collected simultaneously using a polished Si beam splitter and two Si avalanche photodiodes (APD's), connected to two Tektronix 7912A/D waveform digitizers. The digitized data was transferred to a laboratory computer for convenient data acquisition and analysis. The rise time of the entire system was ~ 1 ns.

The computerization of the experiment greatly facilitated the data analysis, in that the baseline could be conveniently subtracted, and the data properly normalized by taking an average reflectivity trace on the unirradiated sample and comparing this with the known value of the reflectivity of either Si or Ge at 632.8 or 1152 nm. In addition, it was noted that the 1152-nm probe-laser intensity was modulated with a 2-ns oscillation (probably due to longitudinal mode beating), which could be effectively eliminated by Fourier transforming the TRR, filtering out the spurious oscillation, and then Fourier transforming back to get the filtered TRR. In some cases, the computer was used to perform energy-discriminated signal averaging; each TRR trace was loaded into the computer, along with the energy density measured with the microjoule meter, and the signal averaging performed only for traces of similar energy density.

Since all the TRR data was stored on a floppy disk, it was possible to have the computer perform the calculations necessary for the determination of parameters such as the melt duration and the time of the onset of melting. To determine the onset of melting, a linear least-squares fit was obtained for the reflectivity versus time (1) for times less than the melt onset and (2) for times just above the melt onset but before the reflectivity reaches the value for the high-reflectivity phase. The intercept of these two lines gives an accurate determination of the time of the onset of melting and for the reflectivity at this time. The time of the end of melting was determined in a similar manner, using the reflectivity versus time after the end of the high-reflectivity phase. The melt duration was calculated as the time of the end of the melt minus the time of the onset of melting.

In order to determine the reflectivity of Si and Ge in the hot solid and the liquid phases, self-reflectivity measurements were made. For this experiment, a piece of Supracil quartz was used as a beam splitter. Approximately 5% of the light reflected from each surface of the beam splitter was focused through a converging lens (placed at twice the focal length of the lens from the sample surface) to a fast-response, uv-enhanced phototube (also placed at twice the focal length of the lens from the lens). The reflected light passed through a 100-μm aperture at the photodetector, resulting in a 100-μm spot on the sample surface being imaged onto the photodetector. A 248-nm narrow bandpass filter was also placed in the light path to eliminate any spurious light (such as luminescence from the sample or any of the optical elements). Simultaneously, the TRR of the sample surface was recorded, allowing us to know precisely when the sample surface melted. Because of the small but significant transverse inhomogeneities in the laser beam, the self-reflectivity from different energy densities could not be compared, but it was possible to compare the time-resolved ratio of the reflectivities of Si and Ge for the same energy density. In this way, we were able to determine the ratio of the reflectivities of the hot solid and the liquid for both Si and Ge.

III. RESULTS AND DISCUSSION

A. TRR before melting occurs

Figure 1 shows the 632.8-nm reflectivity of both germanium (top) and silicon (bottom) as a function of time for several different E_l's near the melting threshold. Similar traces were obtained for the 1152-nm reflectivity, but are not shown. The reflectivity of Si at both 632.8 and 1152 nm, as well as Ge at 1152 nm, increases monotonically with time during the laser heating until the surface melts, resulting in a large increase of the reflectivity. The reflectivity of Ge at 632.8 nm first increases and then decreases with time during laser heating (this is not clear from Fig. 1, but becomes obvious on an expanded scale) until the surface becomes molten, when again there is a

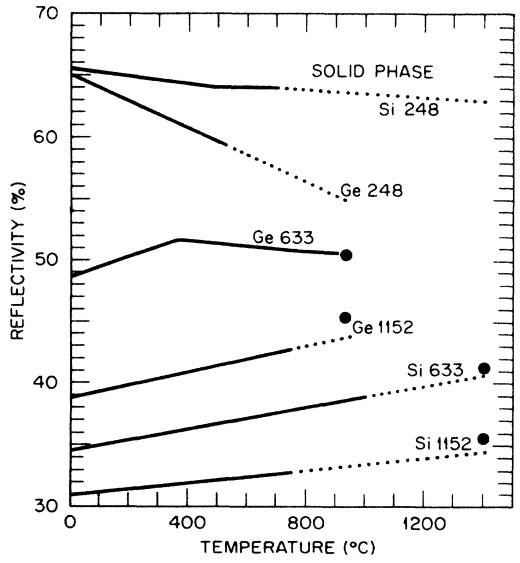

FIG. 2. The reflectivity of Ge and Si as a function of temperature in the solid phase at three different wavelengths (given in nm). The solid lines refer to interpolations of data in the literature (see the text for appropriate references), while the dotted lines refer to linear extrapolations to the melting point of the material. The closed dots refer to the values of the reflectivity obtained at the transition from solid to liquid from this work (see text).

large increase in the reflectivity.

The behavior of the reflectivity of Si and Ge in the solid phase is due to heating by the laser pulse. Figure 2 shows the reflectivity of Si and Ge in the solid phase at 1152, 632.8, and 248 nm as a function of temperature. The solid lines represent interpolations of data found in the literature, while the dotted lines represent linear extrapolations of this data. The data for Si and Ge at 1152 and 632.8 nm are from Jellison and Burke,[13] while the data for Si at 248 nm are from Francois *et al.*,[14] and the data for Ge at 248 nm are from Viña *et al.*[15] The dots are measurements of the reflectivity just before the onset of the high-reflectivity phase, and are placed at the melting temperature of the material (Si: 1410 °C; Ge: 937 °C).

As can be seen from Fig. 2, the dots representing the reflectivity just before the onset of melting lie above the extrapolated values of the reflectivity of the hot solid at the melting point of both Si and Ge. This can be interpreted in several different ways, including the following: (1) The solid is superheated $\sim 200 \pm 150$ °C for Si and $\sim 300 \pm 200$ °C for Ge before the onset of melting or (2) the extrapolation of the temperature-dependent reflectivity is not linear, as assumed. In these experiments, no significant dependence of the reflectivity just before the onset of melting on energy density was observed.

B. TRR just above the melting threshold

Many of the traces shown in Fig. 1 correspond to energy densities just above the melting threshold. Two observations can be made from the data presented in Fig. 1, as well as many other traces not shown: (1) The maximum reflectivity increases with increasing energy density from the value expected for hot solid Si or Ge at the melt threshold (0.65 J/cm^2 for Si and 0.32 J/cm^2 for Ge) to that expected for the liquid. This transition does not occur abruptly, but rather over a finite energy density range; full melting does not occur until E_l is $\sim 25\%$ greater than threshold. (2) The duration of the partial melt (see Sec. II for the definition of melt duration) undergoes a discontinuous jump with increasing energy density; no melt durations less than 20 ns were observed for laser-irradiated Si, or less than 25 ns for laser-irradiated Ge. For energy densities just above the melting threshold, the melt duration is independent of energy density.

This behavior has previously been reported by Jellison *et al.*[11] for excimer laser-irradiated Si. In Ref. 11, it was stated that the one-dimensional melting model[1,2] cannot be used to explain this result, since the melt duration would be expected to approach zero continuously. In this paper we show that the same effect is observed for excimer laser-irradiated Ge. In Ref. 11, it was also pointed out that the discontinuity of the melt duration as a function of energy density is consistent with a partial melting analysis, where the near-surface region can be considered as a mixture of solid and liquid during the melt-in process. This is discussed quantitatively in the next subsection.

C. Time-resolved ellipsometry (TRE)

In Ref. 10, Jellison and Lowndes presented TRE data for Si irradiated with a KrF excimer laser. From ellipsometric measurements, it is possible to determine properties of the reflected light other than the magnitude; in particular, the phase difference between r_s and r_p (Δ) and the magnitude of r_p/r_s ($\tan\psi$) can be measured, where r_s and r_p are the Fresnel reflection coefficients perpendicular and parallel to the plane of incidence, respectively. Likewise, the polarized reflectivities R_s and R_p can be determined from the TRE experiments. The additional parameters available from a TRE experiment place valuable constraints on the interpretative model.

If the melt-in process is assumed to be one-dimensional with a well-defined and sharp melt front separating the liquid surface layer and the solid beneath, there is only one free parameter (the liquid thickness) to use in a calculation of the reflectivity as a function of time. Since TRE measurements give two independent parameters (ψ and Δ), it is possible to calculate two values of the liquid thickness for each time. These values are shown in Fig. 3 for Si irradiated with 0.80 J/cm^2 (just above the melt threshold) and in Fig. 4 for Si irradiated with 1.4 J/cm^2 (well above the melt threshold). Clearly, the liquid thickness calculated from ψ is significantly less than that calculated from Δ, indicating that the simplest model of the melt-in process is not adequate.

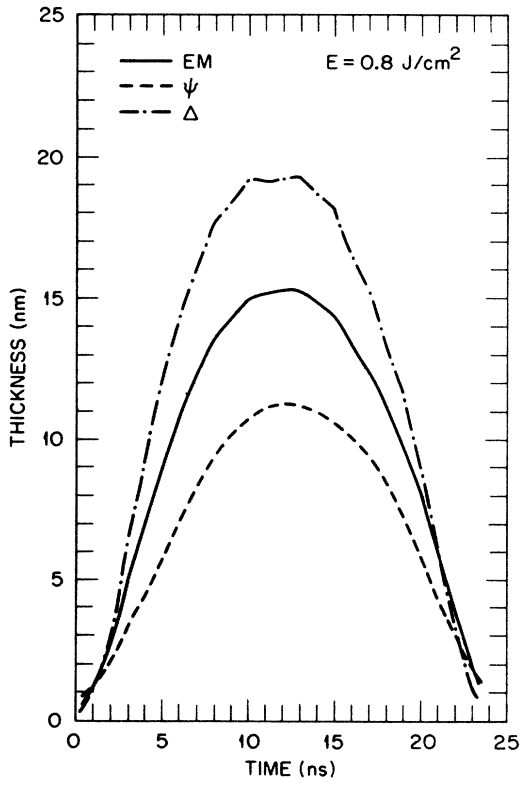

FIG. 3. Thickness of a liquid layer on Si as a function of time during pulsed-laser irradiation at $E_l = 0.8$ J/cm^2 (just above the melting threshold). Time=0 corresponds to the initialization of the melt. The dashed-dotted lines refer to the thicknesses calculated from the ψ vs time and the Δ vs time profiles obtained from time-resolved ellipsometry experiments. The solid line, labeled EM, corresponds to the thickness versus time obtained by the product of the effective medium thickness times the fraction of liquid (see text).

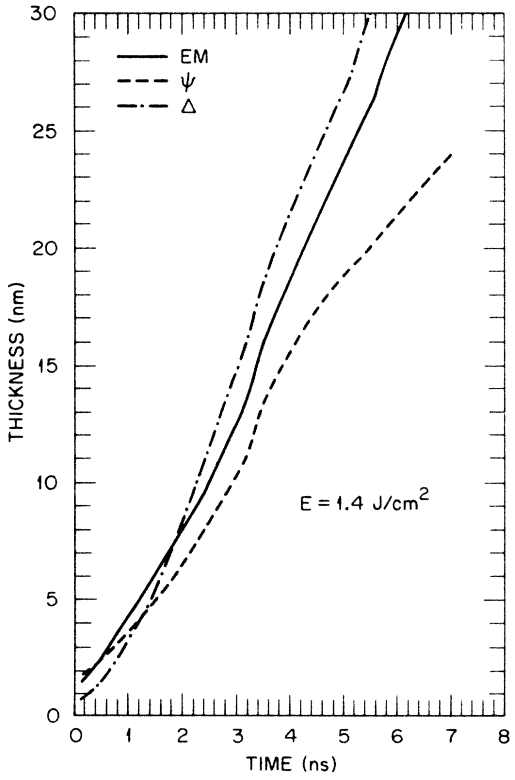

FIG. 4. Same as Fig. 3, but for $E_l = 1.4$ J/cm^2, well above the melt threshold.

A more realistic model is one in which the near-surface region is assumed to consist of a layer of liquid and solid coexisting (slush) just as melting begins. If the near-surface region is modeled as an effective medium,[16] with liquid and solid coexisting, two free parameters (the thickness of the effective medium layer D and the fraction of solid in the liquid layer F_s) can be determined from the TRE parameters ψ and Δ as functions of time; the results are shown in Fig. 5(a) for Si irradiated with 0.8 J/cm^2 and in Fig. 6(a) for Si irradiated with 1.4 J/cm.^{2} With values of D and F_s determined, the reflectivities R_s and R_p can be calculated and compared with experimental values determined from the TRE experiments. These comparisons are shown in Figs. 5(b) and 6(b) and show that this model is internally consistent. From the product $(1-F_s)D$, the effective thickness of the liquid can be obtained and is shown here in Figs. 3 and 4 by the solid line labeled EM.

For Si irradiated with 0.8 J/cm^2, Fig. 5(a) shows that F_s decreases continuously to a value of ~ 0.2 at 12 ns after the onset of melting, when it starts to increase again to a value of 1 at 24–25 ns after the onset of melting. During this time the thickness of the effective medium layer remains relatively constant at ~ 20 nm. For the case of Si irradiated with 1.4 J/cm^2 (Fig. 6), the fraction of solid decreases continuously to 0, at ~ 7 ns after the onset of melting. The effective medium depth increases to ~ 12 nm, stays at this value for ~ 2 ns, and then continues to increase with time. Therefore, even for energy densities

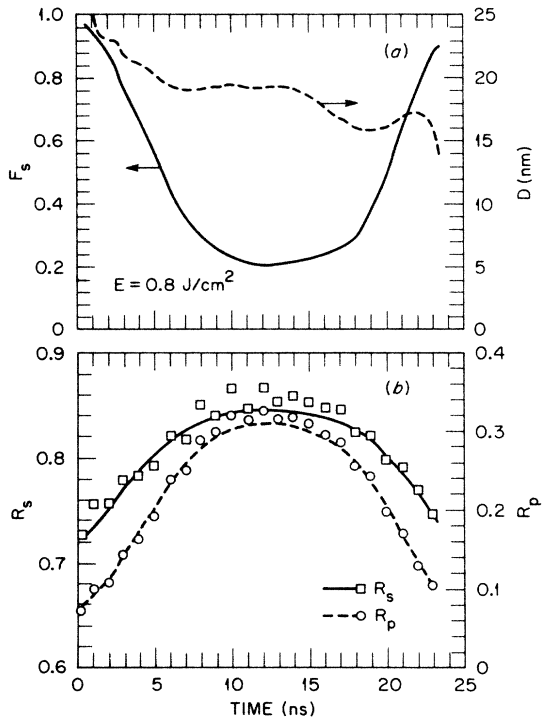

FIG. 5. (a) Effective medium thickness D and fraction of solid F_s calculated from ψ and Δ using the effective medium theory (see text) for Si irradiated with KrF excimer laser pulses $E_l = 0.8$ J/cm^2. (b) The reflectivities for light polarized parallel (R_p) and perpendicular (R_s) to the plane of incidence; the lines refer to R_s and R_p calculated from the effective medium thickness D and the fraction of solid F_s given in (a) above, while the points refer to actual experimental data points. Time=0 corresponds to the initialization of the melt.

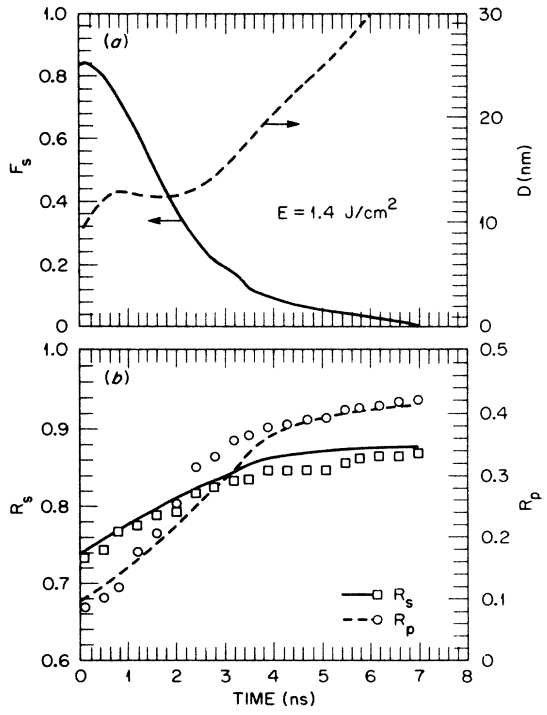

FIG. 6. Same as Fig. 5, but for $E_l = 1.4$ J/cm^2.

sufficient to create a long-lived melt (~ 85 ns in this case) it takes an appreciable amount of time for the near-surface region accessible to the 632.8-nm probe beam to melt completely.

The picture suggested by our effective medium model is one in which the liquefaction of the near-surface region occurs as a bulk process, with liquid inclusions forming within the top 20 nm and then growing as more laser energy is absorbed. Phenomena similar to this have been reported and discussed frequently in the literature[17] for both cw and pulsed-laser irradiation of Si and Ge. Combescot *et al.*[18] have emphasized the importance of differences between the reflectivities and absorption coefficients of the liquid and the solid in explaining inhomogeneous melting, where the interaction of the coherent laser radiation with surface waves is thought to play a role. We note here, however, that at the 248-nm wavelength of the KrF excimer laser, the absorption coefficient and the reflectivity of Si change very little on melting and that excimer laser radiation is not highly coherent. We suspect that the inhomogeneous melting apparently present in our experiments is due to one or more of the following: (1) inhomogeneities in the spatial distribution of the laser radiation; (2) microscopic imperfections of the sample surface; and/or (3) the phase nucleation process itself.

One limit that the model used here places on the geometry of the liquid inclusions is that they must be smaller than the wavelength of the probe light used (632.8 nm), since the effective medium approximation assumes coherent reflections. If they were larger than the wavelength of light, another model, based on incoherent reflections would be used. We also attempted to fit the data with this model, and were unable to obtain convergence, indicating that the model based on incoherent reflections was not reasonable. The effective medium model used here still represents a simplification of the real situation during laser melt in. A more realistic model would treat the near-surface region with several layers, each described by a fraction of solid and a thickness. However, it would not be possible to determine these extra parameters from the TRE measurements, since there are only two measured parameters ψ and Δ.

D. The time of the onset of melting and the melt duration

Two parameters that can be determined from TRR measurements for comparison with melting-model calculations are the melt duration and the time of onset of melting. The time of the onset of melting will be sensitive only to the optical and thermal properties of the solid (including the temperature dependence), while the melt duration, particularly for long melt durations, will be sensitive primarily to the optical and thermal properties of the liquid. The resulting values of the melt duration for both Si and Ge irradiated with a KrF excimer laser are shown in the top panel of Fig. 7, while the time of the onset of melting is shown in the bottom panel of Fig. 7. For energy densities well above the melting threshold, the melt duration increases monotonically with energy density for both Si and Ge, with the increase being much larger for Ge than for Si. The lines give the results of melting-model calculations described in Sec. IV. There is good agreement between the measured and calculated melt durations and times of onset of melting for both Si and Ge.

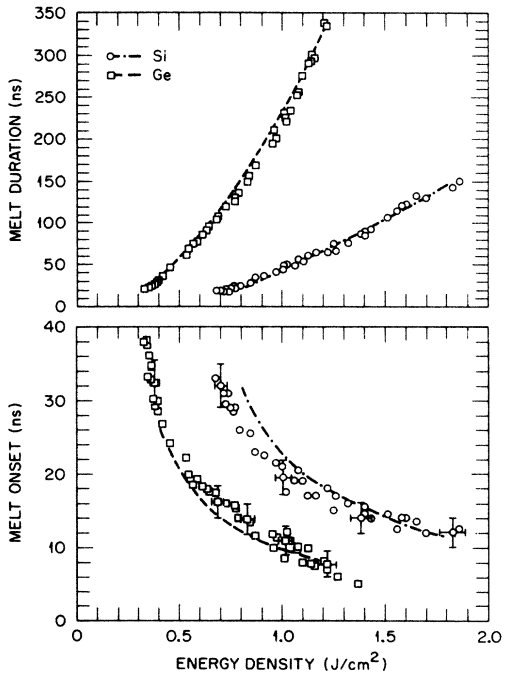

FIG. 7. The melt duration (top) and the time of the onset of melting (bottom) as a function of irradiation laser-energy density for both Si and Ge. The lines represent the results of melting-model calculations, while the data points indicate some of the experimental results.

E. Optical properties of the liquid

It is possible to obtain the values of the reflectivity in the liquid from the TRR data; the values are shown in the bottom panel of Fig. 8 for both Si and Ge by the filled-in data points. The values of the reflectivity determined from the data of Shvarev *et al.*[9] for Si and Hodgson[19] for Ge are shown in the bottom panel of Fig. 8 by the open circles (Si) and the open squares (Ge). Values of the reflectivity at 248 nm ($=5$ eV) are also shown by filled-in data points, determined by comparison of the observed melt duration and the melt duration obtained from melting-model calculations (see Sec. IV). For Ge, values of the reflectivity determined from this work and from the results of Hodgson agree. For Si, our values disagree somewhat with the results of Shvarev *et al.* but the value of the reflectivity at 632.8 nm does agree with the value determined from TRE measurements.[10] This discrepancy of our results with those of Shvarev *et al.* is discussed in Ref. 10.

The values of the optical-absorption coefficient (α) for Si and Ge can also be determined from Refs. 9 and 19, respectively, and are shown in the top panel of Fig. 8. As can be seen, α increases with increasing photon energy, and is on the order of 10^6 cm^{-1} for all photon energies for both liquid Si and Ge. There is no disagreement between

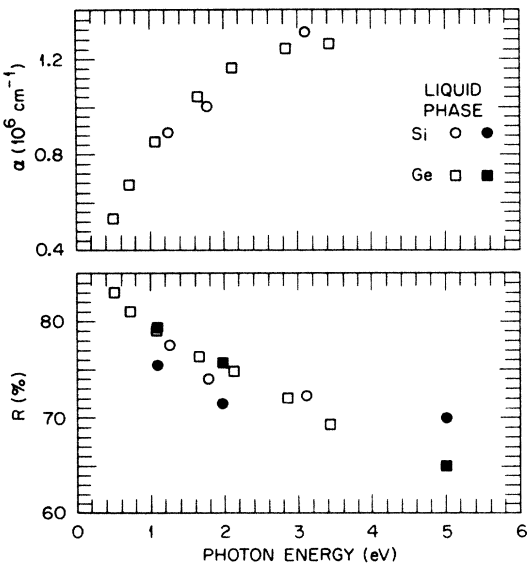

FIG. 8. The optical properties of liquid Si (circles) and Ge (squares) as a function of photon energy. The top panel shows the absorption coefficient (α), while the bottom panel shows the reflectivity (R). The open circles are the results of liquid Si, obtained from Ref. 9, while the open squares are the results of liquid Ge, obtained from Ref. 19. The closed circles and squares are results from this work.

the values of α at 632.8 nm between Refs. 9 and 10. Since α is so large at 5 eV, most of the light is absorbed in the first 200 Å of the liquid and the results of heat-flow calculations will not be strongly dependent on small changes in α. Since α is also on the order of 10^6 cm^{-1} in the solid state at 248 nm for both Si and Ge, it effectively drops out of the heat-flow calculations.

F. Self-reflectivity measurements

The self-reflectivity measurements allow us to determine the ratio of the reflectivities of Si and Ge at 248 nm as a function of time during pulsed excimer laser heating (Sec. II). Because of the uncertainties in determining absolute reflectivities using this method, only relative changes in this ratio during a given laser pulse are considered reliable; the error limits of the ratio are $\pm 5\%$. The following conclusions can be determined from these measurements:

(1) The ratio of the reflectivity of crystalline Ge [R(c-Ge)] to that of crystalline Si [R(c-Si)] decreased $\sim 5\%$ during a 0.30 J/cm^2 pulse (slightly below the melting threshold of c-Ge, but well below the melting threshold of c-Si). Since it is known that R(c-Ge) decreases $\sim 20\%$ in going from room temperature to the melting point, this indicates that R(c-Si) also decreases with increasing temperature.

(2) The ratio of the reflectivity of liquid Ge [R(l-Ge)] to R(c-Ge) is 1.17 ± 0.05, while the ratio R(l-Si)/R(c-Si) is 1.15 ± 0.05, with the reflectivity of the crystalline materials measured near their melting points.

These results can be compared with the average reflectivities of the solid and liquid, determined from comparisons of melting-model calculations with time of onset of melting and melt duration data, discussed in the next section.

IV. MELTING-MODEL CALCULATIONS

In the process of pulsed-laser heating of semiconductors, it is known that the time to convert the energy of electron-hole pair formation to heat is on the picosecond time scale (see Chaps. 4 and 6 of Ref. 1). Since the laser annealing process considered in this paper uses nanosecond laser pulses, it is appropriate to assume that all the absorbed excimer laser light is converted immediately to heat. As a result, the pulse-laser annealing process can be treated by the usual heat-diffusion equation with the laser pulse as a heat source term and with the inclusion of phase change capabilities (see Refs. 1 and 2).

The application of the "melting model" to an actual pulsed-laser annealing experiment is complicated by the lack of information about the temperature dependence of the optical and thermal properties of the material under study. The thermal conductivities of solid Si and Ge have been measured as a function of temperature by many groups, but particularly accurately by Glassbrenner and Slack.[20] However, the thermal conductivities of liquid Si and Ge have not been accurately measured and, therefore, we have employed the Wiedemann-Franz law to obtain the thermal conductivity of both l-Si and l-Ge. Graphs of the temperature-dependent thermal conductivities used in our calculations are given in Chap. 4 of Ref. 1. The temperature-dependent specific heats of solid Si and Ge were taken from the compilation of Hultgren *et al.*[21] The specific heat of the liquid has not been accurately measured, and was assumed to be approximately equal to that of the solid at the melting temperature. (The melt duration is not very sensitive to the specific heat of the liquid.)

The optical absorption coefficients of Si and Ge are also not known accurately at 248 nm, but they are known to be $> 10^6$ cm^{-1} and therefore do not enter significantly into the results of the melting-model calculations. An extrapolation of the results shown in Fig. 8 allow us to assume that $\alpha = 1.5 \times 10^6$/cm for l-Si and $\alpha = 1.3 \times 10^6$/cm for l-Ge. In the solid phase, we have chosen $\alpha = 1.8 \times 10^6$/cm for c-Si and $\alpha = 1.6 \times 10^6$/cm for c-Ge, taken from the room-temperature results of Aspnes and Studna.[22] Since these values are all greater than 10^6/cm, most of the laser radiation will be absorbed and converted into heat in the first 200 Å of the sample; because α is so large, uncertainties of a factor of 2 or more have no significant effect on melting-model calculations.

The reflectivities of Si and Ge at 248 nm ($=5$ eV) are other quantities not known accurately, and unfortunately they do have a significant effect on melting-model calculations. The melt duration and the time of the onset of melting determined from model calculations are particularly sensitive to the reflectivities of the liquid and the solid, respectively. This is particularly true when the reflectivity is large, since the amount of energy coupled into the material is proportional to $(1-R)$; a one-percentage point error in R for $R = 60\%$ results in a 2.5% error in

the amount of energy coupled into the sample. The optical functions of solid Si determined by Jellison and Modine[23] only extend to 4.7 eV and up to 700 °C, but the reflectivity of Si determined by Fancois *et al.*[14] extends to 5.5 eV and up to 700 °C and are plotted in Fig. 2 for 248 nm (=5 eV). The optical functions of solid Ge have been determined by Viña *et al.*,[15] but there is sufficient discrepancy between their results and the results of Aspnes and Studna[22] at room temperature and at 5 eV to question the accuracy of one or both sets of measurements.

The melting-model calculations were carried out using both the HEATING5 computer code[2] and a newly developed code LASER8 (described in detail in Ref. 24). No overheating or undercooling of the solid-liquid interface was assumed. In the calculations described here, the reflectivities of the solid and liquid were adjusted to obtain a good agreement between the calculated and experimentally determined onset of melting and melt duration as a function of laser-energy density. The resulting fits are shown in Fig. 7 and the values of the reflectivities are listed in Table I.

The ratios of the reflectivities in Table I can now be compared with the ratios obtained from the self-reflectivity measurements. From Table I $R(l\text{-Ge})/R(c\text{-Ge})=1.08$, while the self-reflectivity results yield 1.17 for this ratio. However, the self-reflectivity results show the ratio of the reflectivities of the liquid to the solid *at the melting point,* while the ratios obtained from Table I assume average reflectivity in the solid phase. From Fig. 2, we see that the reflectivity of c-Ge decreases from 65% at room temperature to 55% at the melting point. This results in an average reflectivity in the solid phase of 60%, in agreement with the value shown in Table I, and a self-reflectivity ratio at the melting point of 1.18, in agreement with the ratio obtained from the self-reflectivity measurements.

For the case of Si, we get $R(l\text{-Si})/R(c\text{-Si})=1.11$, in reasonable agreement with the self-reflectivity result of 1.15. We do not have reflectivity data extending up to the melting for Si, but for the liquid reflectivity in Table I, the self-reflectivity ratio gives $R=0.61$ for solid Si near melting. From Ref. 14, the reflectivity of c-Si starts at 67% at room temperature, and decreases quickly to 65% as the temperature is increased to 300 °C; therefore, an average reflectivity of 63% for c-Si is quite reasonable.

The use of a one-dimensional melting analysis may be questioned in view of the inhomogeneous melting discussed in Sec. III. In principle this is a valid concern, especially for energy densities near the melting threshold, when the front surface does not become completely molten. However, our definition of the onset of melting is tied to the time the reflectivity just begins the sharp rise from its hot solid value, whereas inhomogeneous melting effects the rate of increase from that value to the high-reflectivity value. Thus the *onset* of melting is not greatly influenced by the inhomogeneities. Near threshold, the melt duration is effected by inhomogeneous melting and the calculations of this quantity do not agree particularly well with experiment until E_l is ~ 0.1–0.2 J/cm^2 above threshold. For Si at $E_l=1.4$ J/cm^2, the calculated position of the melt front agrees very well with the effective medium curve on Fig. 4 and, as Fig. 7 shows, the calculated and measured melt durations are in excellent agreement. Thus there seems little doubt that a one-dimensional calculation is appropriate for most of the E_l range considered here.

TABLE I. The reflectivities of solid and liquid silicon and germanium at 248 nm determined by fitting the calculated values of the melt duration and the time of the onset of melting to the experimental values. The values of the reflectivity in the solid represent an average over the temperature range from room temperature to the melting point.

Material	Solid	Liquid	Ratio
Si	0.63	0.70	1.11
Ge	0.60	0.65	1.08

V. SUMMARY

Time-resolved reflectivity and ellipsometry measurements have been made during pulsed excimer laser irradiation of Si and Ge. From these measurements, we have been able to determine values for the time of onset of melting and melt duration as functions of irradiation energy density. These values were compared with the results of melting-modeling calculations, in which the optical reflectivity of the solid and the liquid were the only adjustable parameters. The values of the reflectivities thus established are in good agreement with the results of self-reflectivity measurements and are given in Table I.

It is possible to obtain the values of the reflectivities of the liquid and the hot solid just before melting at the two probe wavelengths used (632.8 and 1152 nm) from the time-resolved reflectivity measurements. The reflectivities of liquid Si and Ge shown in Fig. 8 are in good agreement with previously reported results for Ge. The minor disagreement with previous results for liquid Si may be due to small errors in the measurements of Shvarev *et al.*,[9] as discussed in Ref. 10. The values of the reflectivities of the hot solid determined from the time-resolved reflectivity measurements are slightly above the values one would expect from an extrapolation of constant temperature measurements, perhaps indicating either a small superheating effect or a nonlinear temperature dependence of the reflectivity.

Near the melt threshold, it has been observed that the melt duration never gets below 20 ns for Si or 25 ns for Ge; furthermore, the maximum reflectivity increases monotonically with energy density over a finite energy density range from threshold (0.32 J/cm^2 for Ge and 0.65 J/cm^2 for Si) to approximately 25% above the threshold. This observation cannot be explained by a simple melt-in model, where the melt front is assumed to start at the front surface and proceed into the material parallel to the front surface. A reinterpretation of time-resolved ellipsometry results indicates that the front surface melts inhomogeneously, where the front surface region consists of a mixture of solid and liquid phases coexisting for some

time. For energy densities just above the melt threshold, the front surface region never becomes fully molten, while for energy densities well above the melt threshold, the melting of the near surface region can take a significant amount of time (7 ns for the case of 1.4 J/cm^2).

ACKNOWLEDGMENTS

This research was sponsored by the Division of Materials Science, U.S. Department of Energy under Contract No. DE-AC05-84OR21400 with Martin Marietta Energy Systems, Inc.

[1]*Semiconductors and Semimetals,* edited by R. F. Wood, C. W. White, and R. T. Young (Academic, New York, 1984), Vol. 23.

[2]R. F. Wood and G. E. Giles, Phys. Rev. B **23**, 2923 (1981).

[3]D. H. Lowndes, G. E. Jellison, Jr., and R. F. Wood, Phys. Rev. B **26**, 6747 (1982).

[4]D. H. Lowndes, Phys. Rev. Lett. **48**, 267 (1982).

[5]D. H. Lowndes, R. F. Wood, and R. D. Westbrook, Appl. Phys. Lett. **43**, 258 (1983).

[6]G. J. Galvin, M. O. Thompson, J. W. Mayer, P. S. Peercy, R. B. Hammond, and N. Paulter, Phys. Rev. B **27**, 1079 (1983); M. O. Thompson, J. W. Mayer, A. G. Cullis, H. C. Weber, N. G. Chew, J. M. Poate, and D. C. Jacobson, Phys. Rev. Lett. **50**, 896 (1983).

[7]W. R. Sooy, M. Geller, and D. P. Bortfeld, Appl. Phys. Lett. **5**, 54 (1964).

[8]D. H. Auston, C. M. Surko, T. N. C. Venkatesan, R. E. Slusher, and J. A. Golovchenko, Appl. Phys. Lett. **33**, 437 (1978); D. H. Auston, J. A. Golovchenko, A. L. Simons, R. E. Slusher, P. R. Smith, C. M. Surko, and T. N. C. Venkatesan, *Laser-Solid Interactions and Laser Processing—1978,* Proceedings of the Symposium on Laser-Solid Interactions and Laser Processing, AIP Conf. Proc. No. 50, edited by S. D. Ferris, H. J. Leamy, and J. M. Poate (AIP, New York, 1979), p. 11.

[9]K. M. Shvarev, B. A. Baum, and P. V. Gel'd, High Temp. **15**, 548 (1977).

[10]G. E. Jellison, Jr., and D. H. Lowndes, Appl. Phys. Lett. **47**, 718 (1985).

[11]G. E. Jellison, Jr., and D. H. Lowndes, Proc. Mater. Res. Soc. Symp. **35**, 113 (1985).

[12]G. G. Devyatykh, E. M. Dianov, N. S. Karpychev, S. M. Mazavin, V. M. Mashinskii, V. B. Neustruev, A. V. Nikolaichik, A. M. Prokhorov, A. I. Ritus, N. I. Sokolov, and A. S. Yushin, Sov. J. Quantum Electron **10**, 900 (1980).

[13]G. E. Jellison, Jr., and H. H. Burke, J. Appl. Phys. **60**, 841 (1986).

[14]J. C. Francois, G. Chassaing, L. Argeme, and R. Pierrisnard, J. Opt. **16**, 47 (1985).

[15]L. Viña, S. Logothetidis, and M. Cardona, Phys. Rev. B **30**, 1979 (1984).

[16]D. A. G. Bruggeman, Ann. Phys. (Leipzig) **24**, 636 (1935).

[17]W. G. Hawkins and D. K. Biegelsen, Appl. Phys. Lett. **42**, 358 (1983); J. E. Sipe, J. F. Young, J. S. Preston, and H. M. van Driel, Phys. Rev. B **27**, 1141 (1983); J. F. Young, J. S. Preston, H. M. van Driel, and J. E. Sipe, Phys. Rev. B **27**, 1155 (1983); J. F. Young, J. E. Sipe, and H. M. van Driel, Phys. Rev. B **30**, 2001 (1984).

[18]M. Combescot, J. Bok, and C. Benoit à la Guillaume, Phys. Rev. B **29**, 6393 (1984).

[19]J. N. Hodgson, Philos. Mag. **6**, 509 (1961).

[20]C. J. Glassbrenner and G. A. Slack, Phys. Phys. **134**, A1058 (1964).

[21]R. Hultgren, P. D. Desai, D. T. Hawkins, D. T. Geiser, K. K. Kelley, and D. D. Wayman, in *Selected Values of the Thermodynamic Properties of the Elements* (American Society for Metals, Metals Park, Ohio, 1973).

[22]D. E. Aspnes and A. A. Studna, Phys. Rev. B **27**, 985 (1983).

[23]G. E. Jellison, Jr., and F. A. Modine, J. Appl. Phys. **53**, 3745 (1982).

[24]G. A. Geist and R. F. Wood, Oak Ridge National Laboratory Report No. ORNL-6242 1985 (unpublished), available from the authors; R. F. Wood and G. A. Geist, Phys. Rev. B **34**, 2606 (1986).